

Study of high-field atomic effects in picosecond laser produced plasmas

J Howe, C Courtois, C D Gregory, I M Hall, N C Woolsey

Department of Physics, University of York, Heslington, York, North Yorkshire, YO10 5DD

D M Chambers

AWE Ltd., Aldermaston, Berkshire, RG7 4PR, UK

E Förster, I Uschmann

Institute of Optics and Quantum Electronics, University of Jena, 07743 Jena, Germany

O Renner

Institute of Physics, Academy of Sciences CR, 18221 Prague, Czech Republic

Main contact email address: jh222@york.ac.uk

Introduction

The analysis of spectral line emission is an extremely valuable tool in identifying phenomena and determining the hydrodynamic conditions in high density laser produced plasma¹. Oscillating electric fields within plasma can be diagnosed by the presence of field induced satellite lines to allowed and forbidden transitions². It has been suggested that the intensity of a laser focussing into preformed plasma can be determined by the presence of these satellite transitions³. Here we describe a spectroscopic study of plasmas produced by picosecond duration intense laser interaction and explore the possibility of observing such satellite transitions. In addition, we also report the observation of intensity modulation of the aluminium He β line profile. This observation is based on the analysis of high spatially resolved and high spectrally resolved data and interpreted utilising 1-D hydrodynamic simulations.

Experiment

The experiment was conducted in Target Area 2 at the Astra laser facility. Targets consisting of 200 μm diameter 5 cm long aluminium fibres were irradiated with 800 nm laser pulses with FWHM of 3.4 ps. An off axis parabolic (OAP) mirror was used to focus both laser pulses onto the target with an angle of 10° to the vertical axis. By defocusing the parabola, the on target focal spot varied to give intensities between $7 \times 10^{14} \text{ W cm}^{-2}$ and $3 \times 10^{16} \text{ W cm}^{-2}$. In some cases a secondary pulse, compressed to 50 fs, was introduced along the same optical path to determine if this laser could perturb spectral emission. The focussed intensities of the second pulse varied between $5 \times 10^{15} \text{ W cm}^{-2}$ and $2 \times 10^{18} \text{ W cm}^{-2}$ and were delayed between 50 ps and 400 ps with respect to the picosecond pulse. The experimental geometry is shown in Figure 1. By translating the aluminium fibre through the focal spot and firing the laser at a repetition rate of 2 Hz, up to 100 shots were integrated to make a single recording. The high-resolution, highly dispersive toroidally bent crystal spectrometer (HDTS)⁴ was positioned to record spectral emission parallel to the target surface and spatially resolved perpendicular to the surface. The spectral measurements were recorded with 3 μm spatial resolution having a magnification of the crystal of about 4. The energy dispersed X-ray emission from the plasma was recorded onto a cooled, large area scientific-grade CCD camera fitted with an e2V technologies 16-bit CCD42-90 detector with a pixel size of 13.5 μm . Typical data integration times were approximately 3 minutes. The spectrometer was positioned to disperse two energy ranges with $\sim 0.2 \text{ eV}$ resolution. Firstly, referred to as position A, 1830 eV to 1872 eV containing the $\text{Al}^{+11} \text{ He } \beta$ ($n = 3 - 1$) transition and the neighbouring Li-like dielectronic satellites. Secondly, referred to as position B, the $\text{Al}^{+11} \text{ He } \gamma$ ($n = 4 - 1$), $\text{He } \delta$ ($n = 5 - 1$), and $\text{He } \epsilon$ ($n = 6 - 1$) transitions lying within the energy range 1840 eV to 1835 eV. Using the crystal of quartz (100) with bending radii 1405.5 (in horizontal, i.e. dispersion plane) and 312.8 mm (vertical), the distance between target-crystal and crystal-CCD for position A was

245.6 mm and 1095.1 mm respectively. For position B the distances were 271.7 mm and 1023.3 mm respectively. A magnet and lead shielding was used to prevent hot electrons striking the CCD and to limit hard X-ray bremsstrahlung background.

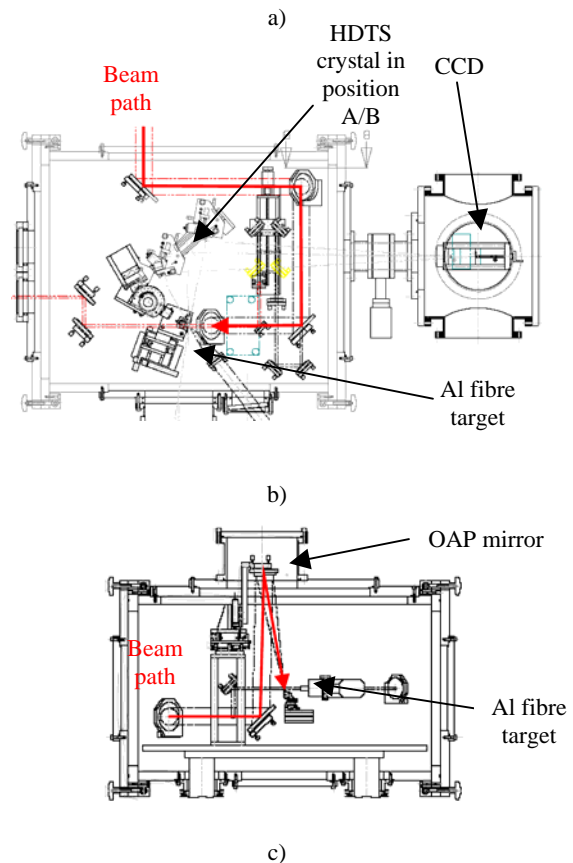
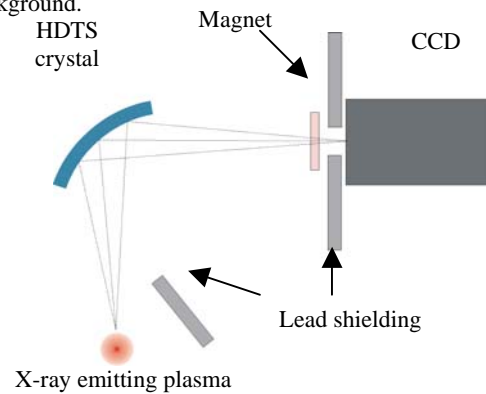


Figure 1. a) Diagram of the spectrometer setup. Cross-sections of the experimental chamber are shown in b) the horizontal plane, and c) the vertical plane.

Results

Figures 2a and 2b show a sample of time integrated raw data at positions A and B respectively. The dispersed photon energy is shown along the horizontal axis, whereas spatial dispersion is shown along the vertical axis. The raw data illustrates the need to integrate over a number of shots; this was required to improve the signal to noise ratio due to the high dispersion (0.8 mm/eV). Spectral information is detected to 0.2 mm above the target surface. Close to the initial target surface the He β resonance lines and Li-like dielectronic satellites are clearly resolved. These satellites are strongly correlated to an excited $1s3p2l$ states populated by collisional processes at high plasma densities³.

Absolute photon intensities can be extracted from this data as the energy dependent crystal reflectivity, CCD detection efficiency, and protective foils transmission are known. This allows direct comparison between measurements. Hot electrons generated during laser-target interaction directly striking the CCD are believed to be responsible for the random speckle, bremsstrahlung and recombination continuum combined with the satellite quasi-continuum represent a source of background seen in the images. By using magnets to pull hot electrons away from the detector, the random speckles were suppressed but not fully excluded.

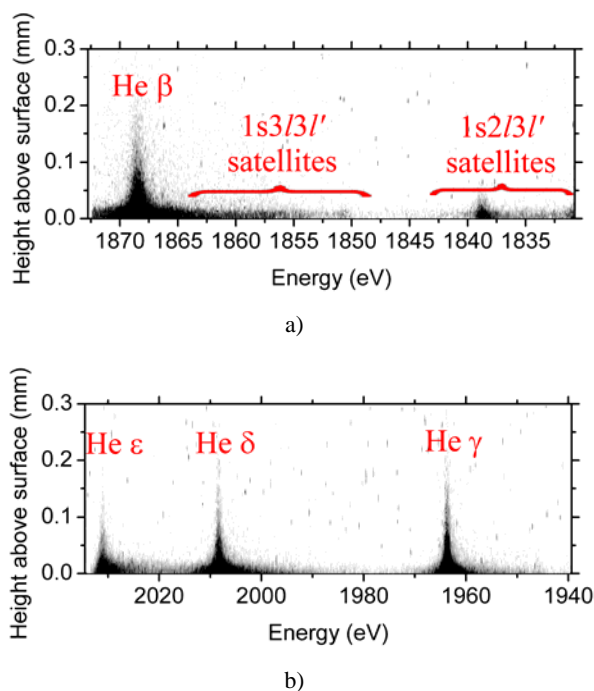


Figure 2. Energy dispersed spatially resolved raw data in the range a) 1830 eV to 1872 eV, and b) 1940 eV to 2035 eV.

Spectral traces are extracted from data such as Figure 2 by averaging over 6 μm in plasma extension above the target. This is repeated at a number of positions above the target surface. An example is shown in Figure 3. Here spectral line profiles of the He β transition taken at 15 μm above the target surface from two measurements are compared. The red curve shows the line profile typical of 3.4 ps duration pulse at $3 \times 10^{16} \text{ W cm}^{-2}$. The resonance line ($1s3p^1P_0 \rightarrow 1s^2^1S_0$) at 1868.7 eV is clearly seen. The black curve shows this transition when driven with an additional 50 fs pulse delayed by 100 ps and focussed at $2 \times 10^{18} \text{ W cm}^{-2}$. It is evident that line emission is stronger when both the prepulse and the main pulse are present. A dip in the line shape observed close to 1869.2 eV is ascribed to absorption phenomena. The three narrow peaks at low energy are due to direct hot electron impacts on the CCD. These hot electron impacts were consistently observed when using the 50 fs, pulse at high intensity.

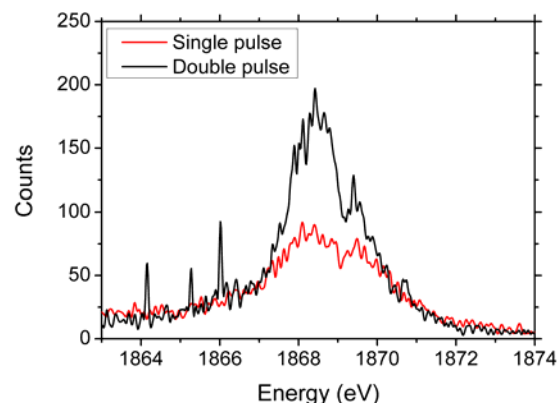


Figure 3. Cross sections of the He β line profile taken at 15 μm above the target surface.

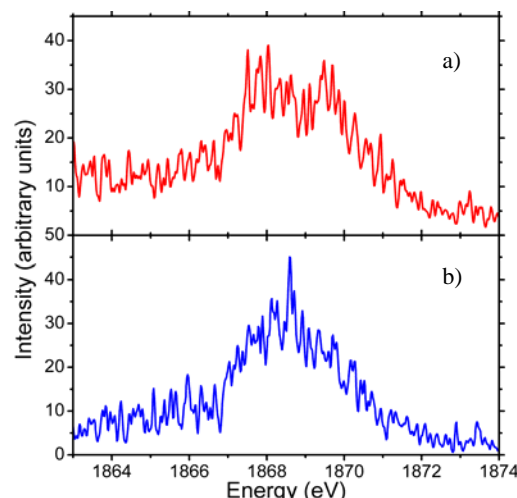


Figure 4. Cross section of the He β line profile taken at 3 μm above the target surface. Laser intensity on target is a) $3 \times 10^{16} \text{ W cm}^{-2}$, and b) $7 \times 10^{14} \text{ W cm}^{-2}$. Notice the modulation intensity decreases with lower laser intensity.

One of our objectives was to look for so called laser induced satellites features. These satellites should be symmetrically displaced about forbidden spectral transitions, shifted by the laser photon energy⁵. Direct comparison of spectral cross-sections obtained using the picosecond pulse and a combination of picosecond and femtosecond pulses indicates that these satellites were not observed. This is likely to be due to the weak emission in these satellites compounded by the short duration of the femtosecond pulse. This pulse also must interact with a sizable preformed plasma.

Of particular interest are the intensity modulations on the He β line profile. These modulations are observed when using the picosecond duration pulse. Figure 4 shows two spectral line profiles of the He β transition of a 3.4 ps duration pulse at $3 \times 10^{16} \text{ W cm}^{-2}$ and $7 \times 10^{14} \text{ W cm}^{-2}$. Modulations, above the noise level, are clearly seen on these line profiles. These modulations are particularly intense close to the target surface, and observed to extend above the target surface in each case. Notice the modulation intensity decreases with lower laser intensity. At greater heights above the target surface the modulations reduce in amplitude in comparison to the integrated resonance line emission and the spacing between neighbouring modulations increases, as illustrated in Figure 5. The modulation intensity reduces in both the red and blue wings of the spectral line. The modulations have been observed on a number of measurements. These measurements show that the features are reproducible and in addition are laser intensity dependent.

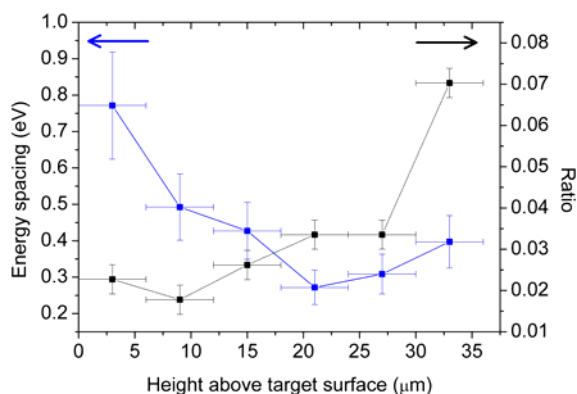


Figure 5. Ratio between modulation amplitude and integrated resonance line emission (right axis), and spacing between modulations (left axis) versus height above the target surface.

As the spectral measurements are spatially resolved but time integrated we have used the 1-dimensional Lagrangian hydrocode MED103⁶⁾ in conjunction with the atomic physics code FLY⁷⁾. MED103 was used to calculate time histories of the plasma for a number of fixed heights above the target surface. These time histories were used with FLY to predict the time of peak He β emission at these heights. We infer the spatially resolved electron temperature and density at peak He β emission. These calculations are shown in Figure 6. It is assumed the modulations observed in the spectral data occur at the time of peak He β emission. If this assumption is valid the simulations suggest the modulations are present in regions where the electron density exceeds the critical density ($1.7 \times 10^{21} \text{ cm}^{-3}$) and *during* the time of laser-plasma interaction. This suggests that the modulation intensities may be dependent on the absorption of the laser energy in regions of different plasma densities. The simulations show that the period of peak He β emission at heights above 20 μm is not well defined. The duration of He β emission at heights up to 3 μm above the surface is approximately 5 ps. At heights above 20 μm the duration of emission extends to approximately 9 ps. The slightly variable plasma parameters corresponding to this extended emission period may smear the modulation contrast.

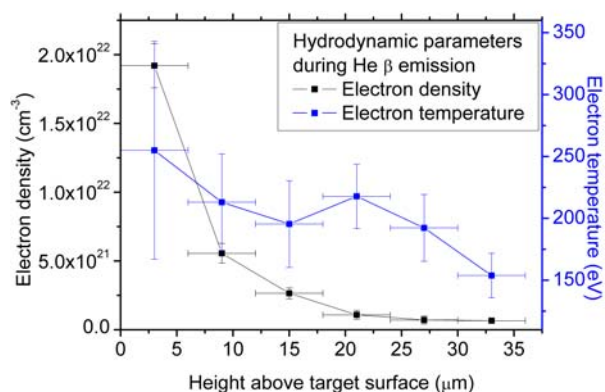


Figure 6. Results of MED103 hydrodynamic simulations coupled with the atomic physics code FLY.

Conclusions

High-resolution aluminium K-shell spectral data have been obtained from single (picosecond) and double (picosecond and femtosecond) pulse experiments. To improve the data signal to noise multi-shot data integration was necessary. Comparison of the single and double pulse data show that enhanced line emission of the helium-like resonance lines is observed due to the action of the second femtosecond pulse. Furthermore, analysis also indicates that the laser induced satellite lines are not observed. This is likely to be due to weak satellite emission and the time-integrated nature of data. Regular intensity modulations on the He β line profile are observed at spatial positions close to the target surface. Hydrodynamic simulations suggest that these features occur during the laser-plasma interaction and at electron densities that exceed the critical density. The origin of these modulations and the dependence on laser and plasma conditions are currently being studied.

References

1. H. R. Griem, Principles of Plasma Spectroscopy
2. M. Baranger and E. Mozer, Phys Rev., 123, 25, (1961)
3. A. Vinogradov and E. Yokov, Sov. J. Quant. Elec., 3, 163, (1973)
4. I. M. Hall *et al.*, CLF Annual Report, 197, (2003/2004)
5. F. B. Rosmej *et al.*, J. Phys. B: At. Mol. Opt. Phys., 31, 921, (1998)
6. A. Djaoui and S. J. Rose, J. Phys. B, 25, 2745, 1992
7. R. W. Lee and J. T. Larson, JQSRT, 56, 535, (1996)